Variability of bridge deck vibrations due to traffic loading

F. Besseling [1,2], P.T. Kockelkorn [1], J. de Bruijn [2], E. Lourens [1]

[1] Delft University of Technology, the Netherlands

[2] Witteveen+Bos Consulting Engineers

Bridges are key objects in infrastructure networks. Many large bridges in Western Europe were constructed in the 50s and 60s of the past century, and are therefore beyond their design lifetime. Moreover, increased traffic loads often exceed the design capacity. Structural health monitoring can be employed for damage detection and risk management for structures of which the capacity cannot be proven to meet the Eurocode design requirements. When employing vibration-based damage detection methods for monitoring the structural health of bridges, it is often possible to increase the data features' sensitivity to damage by focusing on local as opposed to global vibrations. This increased sensitivity, however, comes at a cost: by moving towards the higher frequency ranges and more local behaviour, the effects of operational and environmental variability on the data become increasingly pronounced. Some form of data normalization needs to be employed in order to reduce this variability in the damage-sensitive features extracted from the monitoring data. To effectively design such normalization strategies, a better understanding of the nature of operational and environmental variability is necessary. This paper presents the results of a study focussing on operational variability, based on a long-term monitoring campaign at the Haringvliet bridge, a steel box-girder bridge in the Netherlands. An analytical model is constructed to study the variations in the measured response, by comparing model vibrations to measured vibrations. The influence of vehicle configuration and speed on the vibrations are demonstrated.

Key words: SHM, bridge monitoring, vibration-based, operational variability

1 Introduction

Vibration-based damage detection of bridges uses the dynamic response of the structure to generate information on possible deviations in structural behaviour, which may be associated with structural damage. The system that generates the measured dynamic responses, however, does not only include the bridge structure, but also the traffic on the bridge. In fact, the vehicles on the bridge generate the main dynamic loading on the bridge, but are also a part of the system that responds to this loading. This causes a complex problem in which both the system and the loads are highly time-variant. Within this context, the present study focusses on a specific subtask, namely creating a better understanding of the operational variability due to traffic loads. The results of this study follow from a long-term measurement campaign of two adjacent bridge deck segments of the Haringvliet bridge. The measurement configuration allowed the authors to compare the measured dynamic response of multiple individual sensors, and to analyse the response of groups of sensors, both contributing to a better understanding of the nature of bridge deck vibrations. In addition to this, a simplified semi-analytical model was developed for simulating dynamic bridge deck response due to a dynamic moving load triggered by an uneven road surface. The goal of the model was to aid in understanding the observed bridge deck vibrations for typical traffic load configurations. By comparing the bridge deck response calculated by the model to actual measurement data, a better understanding of the nature and origin of bridge deck vibrations is created.

2 Haringvliet bridge project

2.1 Haringvliet bridge

The Haringvliet bridge is a steel box-girder bridge. Its total length is 1220 metres, with ten similar sections that span 106 metres each, and a section for a movable bridge on the north side, allowing maritime traffic to pass the Haringvliet. The bridge is located south of Rotterdam and forms an important link in the A29 highway, connecting Rotterdam to the South. Figure 1 shows the bridge and its position within the highway network south of Rotterdam. The bridge consists of a hollow steel box section that runs longitudinally along the bridge. Diagonal struts support the cantilever deck plate on either side. Transverse beams are equally spaced along the length of the bridge sections with, between them, stiffeners supporting the bridge deck. Figure 2 shows a structural cross section of the bridge. The bridge has five lanes of traffic, two highway lanes in each direction, with an extra side lane designated for local low-speed traffic. The road surface consists of an asphalt layer on the bridge deck. The traffic, and thus the loading on the bridge, is not symmetric over its width. The southbound traffic is situated on the westward cantilever deck plate of the bridge, while the northbound traffic drives on the centre of the bridge. The local low-speed lane is located on the eastern cantilever deck plate. At the time of the measurement campaign a temporary closure of the middle deck section was established and a speed limit of 50 km/h was imposed.

The bridge was opened in 1964 and has been in service for nearly 60 years. Aged steel bridges appear to be prone to fatigue damage in welded connections (De Jong, 2006, Ya et al., 2011), especially when traffic loads have increased. This also applies to the Haringvliet bridge where fatigue cracks have been identified in the bridge deck structure.

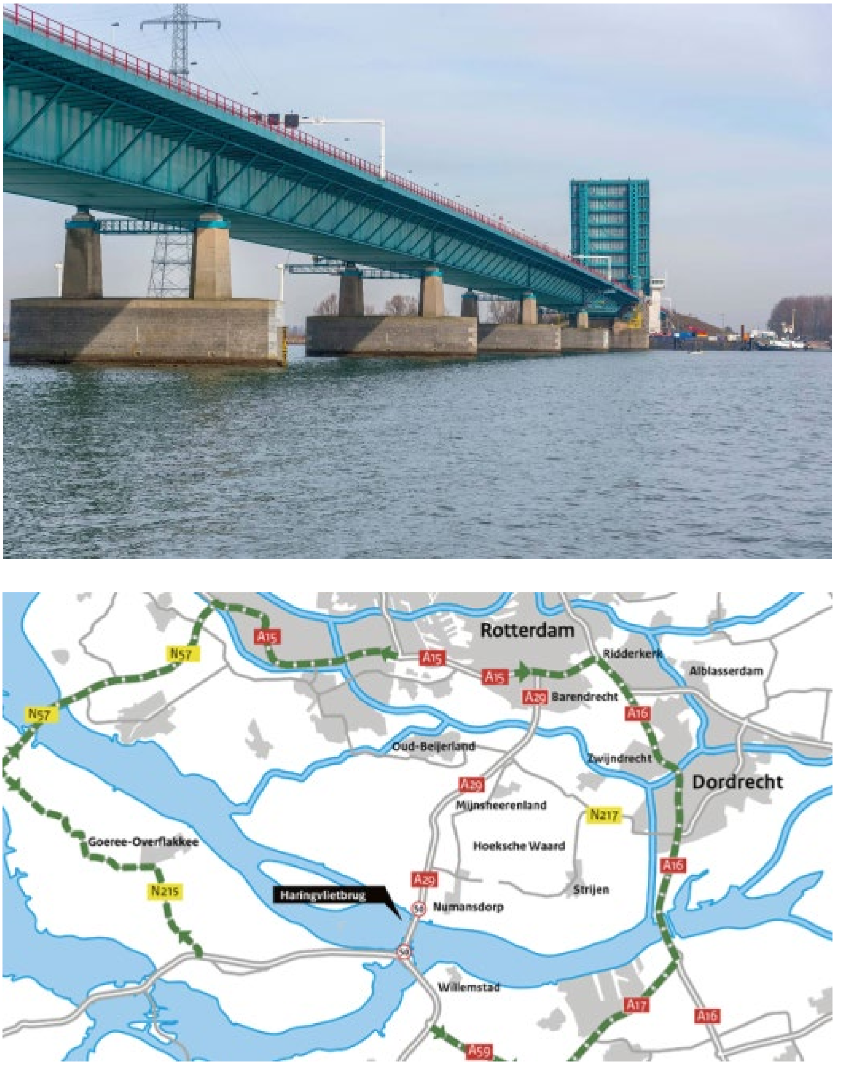

Figure 1. Haringvliet bridge and its location in the highway network south of Rotterdam

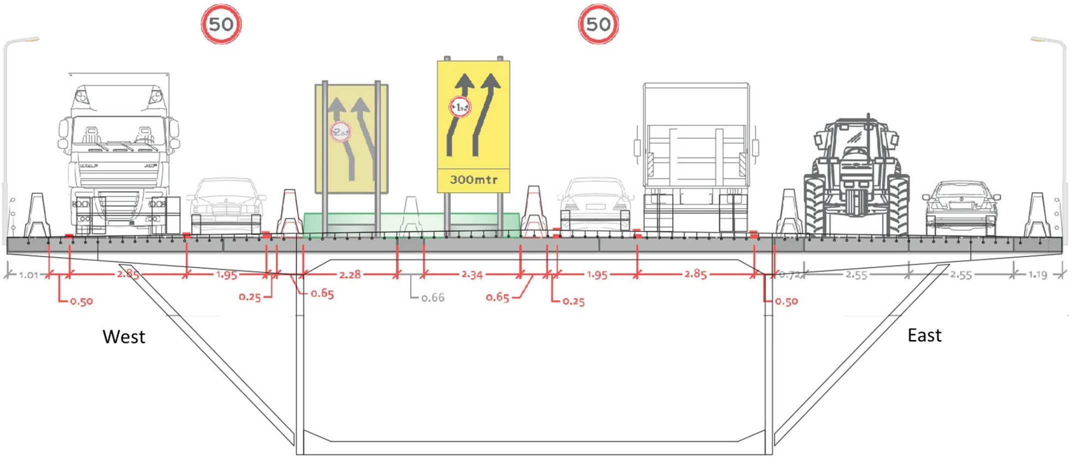

Figure 2. Haringvliet bridge structural cross section at the location of the sensor setup

2.2 ***Vibration-based structural health monitoring***

Structural health monitoring (SHM) as employed in aerospace, mechanical and civil engineering involves monitoring structural behaviour over time and diagnosing potential issues related to the structure's health based on the monitoring data. The aim of SHM here is to timely identify anomalies and incorporate asset data in asset management, in order to achieve higher availability of structures and optimize maintenance and repairs.
Vibration-based structural health monitoring (Deraemaeker, 2012) comprises a subcategory of structural monitoring where the nature of structural vibrations is analysed based on sensor data in order to identify the condition of a structure. Research in this field aims to link anomalies in dynamic behaviour of the structure to damage or to changes in structural capacity. Early identification of damages, e.g. minor cracks in a stage before structural safety becomes critical, requires a sensitive monitoring system. However, environmental and operational variability (EOV) are known to affect the vibration response as well (Deraemaeker A. R., 2008) (Sohn, 2017). EOV effects are in fact masking variations of structural response resulting from damage. Data normalisation methods to correct monitoring data for EOV effects have been extensively researched, aiming to differentiate between structural degradation and normal variations of the measured structure response (E. J. Cross, 2012). Effective data normalisation, however, still appears to be a problematic (Maes, 2022). The work presented in this paper aims to contribute to a better understanding of specifically *operational* variability due to traffic on steel bridges, in order to benefit the development of effective data normalization methods in the future.

Previous work focused on environmental variability, revealing interesting insights into the complexity of thermal effects in steel bridges. The interested reader is referred to (Kortendijk, 2021).

3 Measurement campaign

3.1 Sensor setup and data acquisition

The sensor setup is shown by figure 3. The setup for the measurement campaign was developed to analyse bridge deck vibrations in two adjacent deck segments of the deck, spanning above the steel box girder between 3 transvers beams separated by 2.192 m. The segments were located at midspan of the 108 m bridge main span.

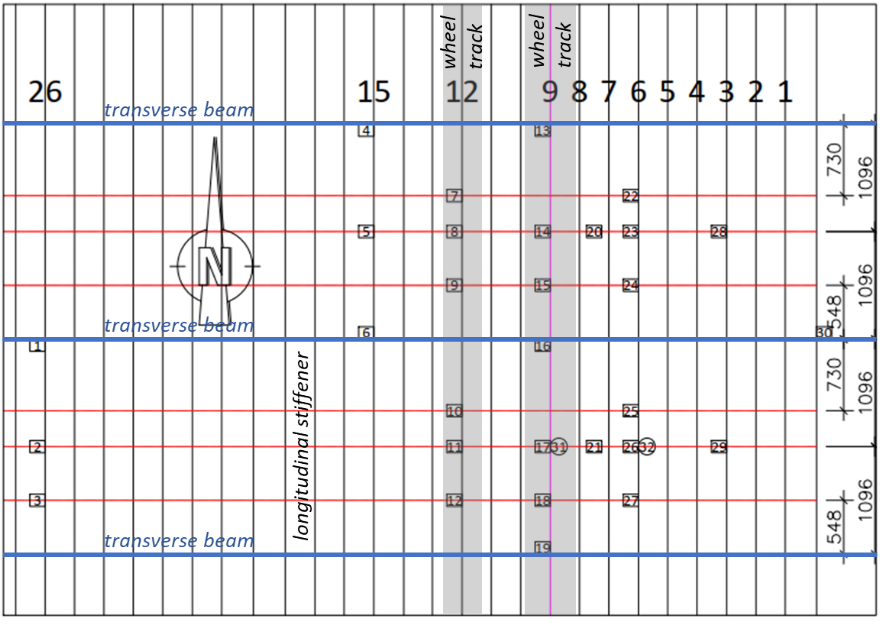

Figure 3. Sensor configuration of the two adjacent deck segments, vertical lines 1 - 26 indicate the deck longitudinal stiffeners spanning 2.096 m between the transverse beams (stiffener 1 is situated adjacent to the East box wall, stiffener 26 below the temporarily closed deck section)

Bridge deck vibrations were measured by 32 accelerometers. The data acquisition unit was of type NI CompactRIO. The sensors were placed such that both the bridge deck response underneath the wheel tracks as well as the response of the 'unloaded' deck (the temporarily closed deck section, as indicated in figure 2) were recorded. Given the configuration of the traffic lanes on the bridge (figure 2), wheel tracks are projected roughly above stiffener 9 and 12, indicated by grey shading. Stiffener 9 is situated below the west side wheel track of the northbound heavy traffic lane, and stiffener 12 below the east side wheel track of the northbound fast traffic lane. The sensor configuration for the two adjacent deck segments were largely identical in order to be able to investigate consistency and differences in response of different deck segments subjected to the same traffic and therewith largely similar traffic loads.

4 Measurement results and variability of deck vibrations

4.1 Typical passages

Vibration data from the deck sensors were analysed with the aim to classify signals into groups corresponding to 'typical' vehicle passages. Vibration signals were analysed both for a full vehicle passage and for the free vibration part of the signal where the vehicle had already passed the deck segment under consideration. An extreme diversity in signal characteristics was, however, observed. Both in the time and frequency domain the signals from the same or supposedly similar sensor locations deviated largely in terms of vibration response. This statement applies to different sensors for the same vehicle passage and for the same sensor for repetitive passages of the same vehicle, reflecting the complex nature of vehicle - bridge deck coupled dynamic response. Two examples illustrating these observations are reported in the following paragraphs.

4.2 Variation between different sensors for the same passage

Figure 4 presents the z-direction vibration signals of sensors 14, 15, 17 and 18 for the same passage of the same vehicle (for sensor positions see figure 3). Sensors 14, 15, 17 and 18 are mounted on the deck at a location approximately below the wheel track. A passing vehicle at this location on the bridge passes sensors 18 and 17 first, before passing sensors 15 and 14 at the next deck segment. The response signals of the sensors clearly show similar frequency domain responses with energy concentrating in a frequency band from around 80 to 95 Hz. The spectra also show concentrations of energy around 15 and 30 Hz. Analysing the time signals, however, results in the conclusion that a very different signal can be obtained from two sensors mounted on 'the same' position of two adjacent deck segments, for the same vehicle passage. We question which underlying parameters, like for example the load history on the deck or the phase of motion of the vehicle, can be pronounced in bridge deck motions which were expected to be similar.

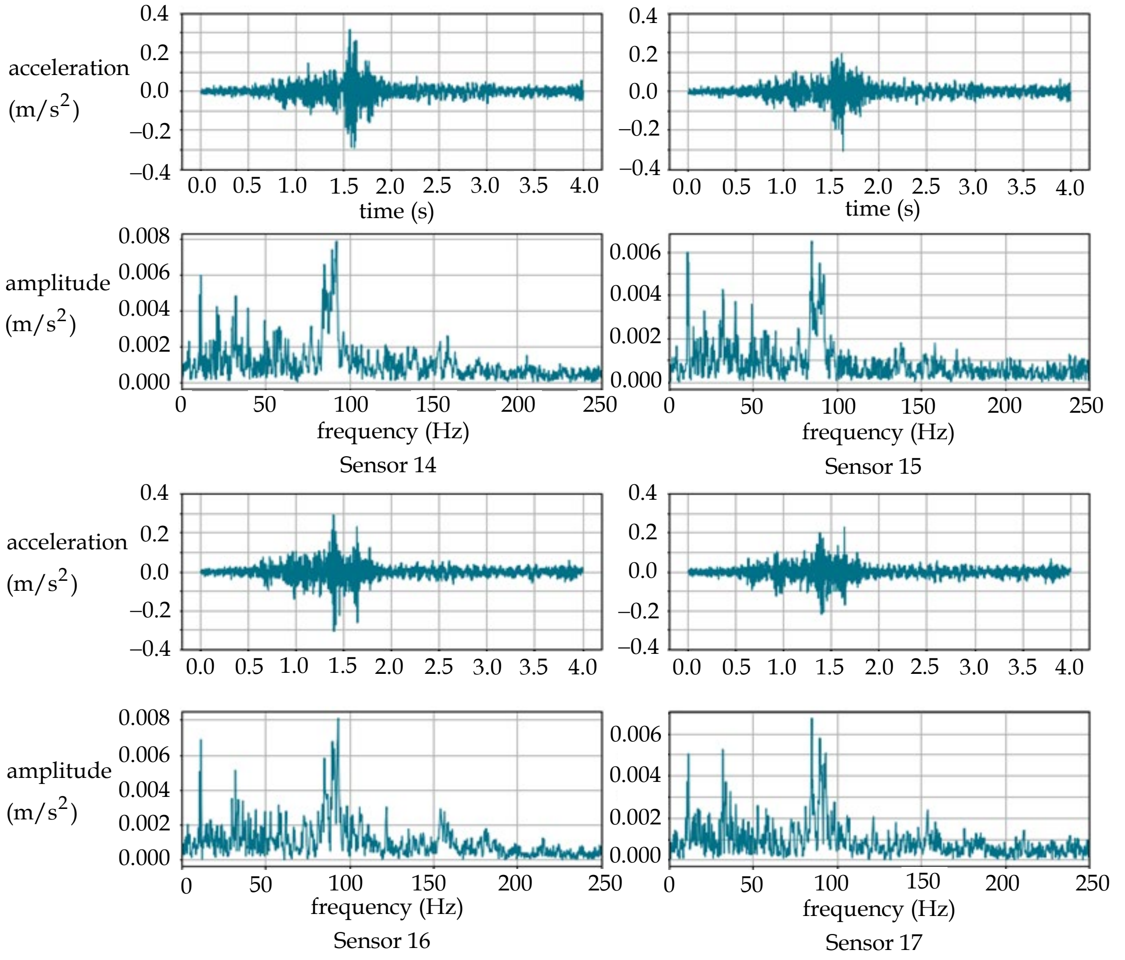

Figure 4. Measured vibration signals (acceleration time signal and frequency spectra) of sensors 14, 15, 17, 18

4.3 *Variations between signals from the same sensor for repetitive passages of the same vehicle*

Following the observed variation among vibration signals of sensors mounted at similar positions on two adjacent deck segments, an experiment has been performed where a) the same car was driven over the instrumented bridge span at different speeds and b) two different cars passed the instrumented span at the same speed. The results of this experiment are presented in figure 5 as frequency spectra of the lateral stiffener response of the stiffener below the wheel track, at midspan of the stiffener. Again, similarities can be observed in the spectra of the recorded signals, e.g. the energy concentration around 250

Hz, but also clear deviations among the signals for supposedly very similar load scenarios are observed. It was concluded that signal characteristics of passages for the same vehicle at the same speed were not necessarily more consistent than signal characteristics for passages of the two different vehicles or for passages with a different vehicle speed.

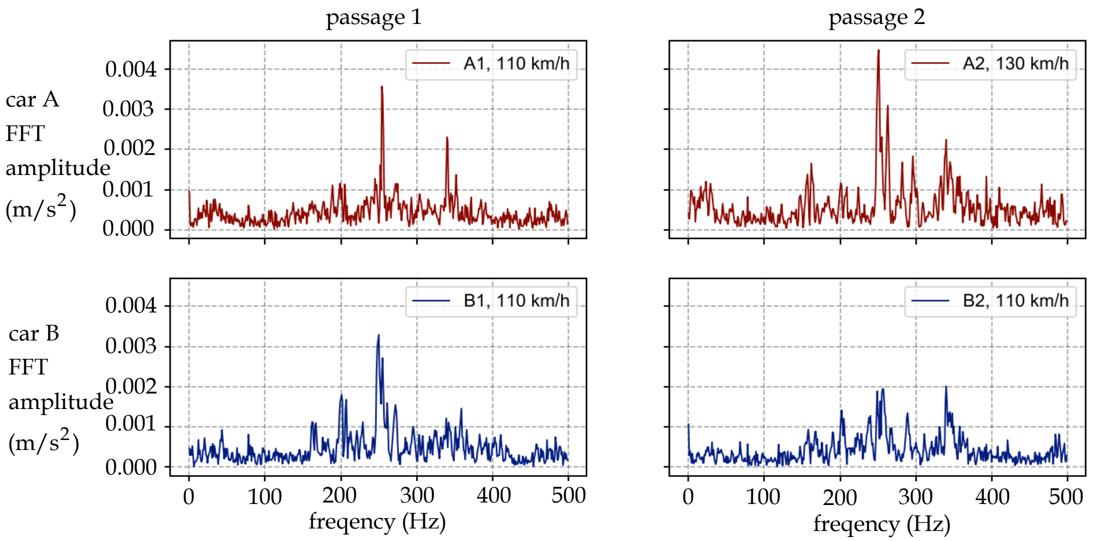

Figure 5. Comparison of stiffener lateral acceleration signal FFT for two passages of two cars at 110 and/or 130 km/h

4.4 Doppler effects

Numerous passages observed at the Haringvliet bridge were found to contain large concentrations of energy in one or two frequency bands, with in each of these bands three distinct peaks in the frequency spectra: cf. figure 6 for an example. All passages considered as belonging to this type were characterized by a large peak acceleration (> 0.2 m/s^2), but the exact locations of the energy concentrations in the frequency domain differed.

The three peaks in these signals could be attributed to the Doppler effect. The typical phenomenon belonging to the Doppler effect can clearly by seen in the spectrogram in figure 9, where as soon as vehicle axles pass the sensor (at t = 1.2 s and 1.4 s), the dominant frequency decreases. With this interpretation the lowest of the three peaks is caused by the vehicle moving away from the sensor, the middle peak when the vehicle is near the sensor (amplification then occurs at the source frequency), and the highest peak when the vehicle is approaching the sensor. The magnitude of the frequency shift depends on the vehicle velocity, the source frequency and the phase velocity. Both an increasing velocity and larger frequency result in a larger frequency shift. The Doppler effect can only exist when a system is time-variant. Since the environmental and structural conditions within the time span of a passage is constant, the Doppler effect in the current system can only be caused by operational variability or, more specifically, the vehicle and its characteristics. These hypothesis are supported by the semi-analytical model results.

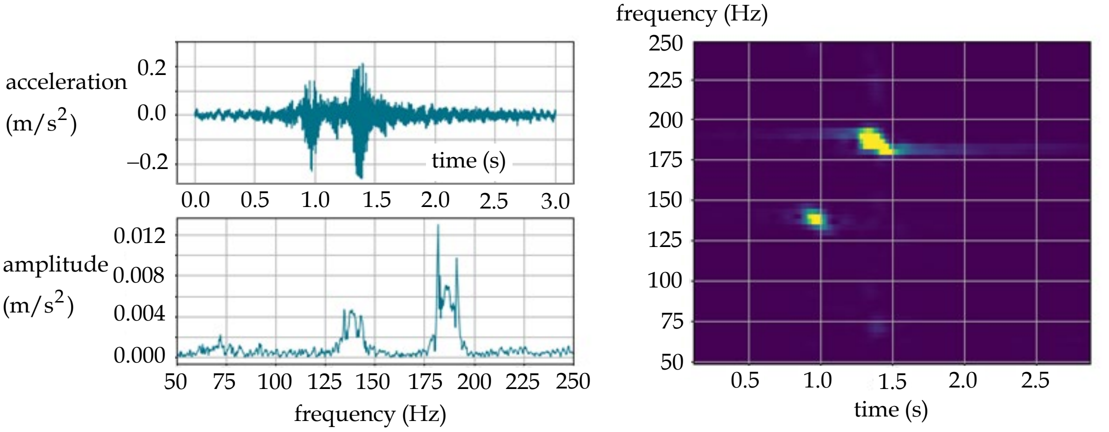

Figure 6. Time history and frequency spectrum (left), and spectrogram (right), of the acceleration response of sensor 17, showing the Doppler effect

4.5 ***Semi-trailer trucks***

Another response signal type that was recurringly observed at the bridge is shown in figure 7, and characterized by multiple high-energy frequency bands and multiple periods showing peak accelerations in the time domain. The classification of this type of passage was done based on the time domain data. By assuming reasonable vehicle velocities and recalculating the time between peaks in the time domain to axle distances, it was possible to compare with typical axle distances of semi-trailer trucks and conclude that these passages likely belong to this type of vehicle. It should be noted, however, that the variation in the frequency spectra of passages classified as semi-trailer trucks was large. This is most likely due to the large variation in trailer truck dimensions, number of wheels, and truckload. Nevertheless, this type of response was often observed. As an example we consider the passage shown in figure 7, characterized by four high-energy frequency bands located at around 70, 90, 130 and 200 Hz. These are frequencies which were observed in the acceleration response of many vehicle passages and relate to natural frequencies of the system. The spectrogram shows that the dominant frequency and amplitude is different for each axle.

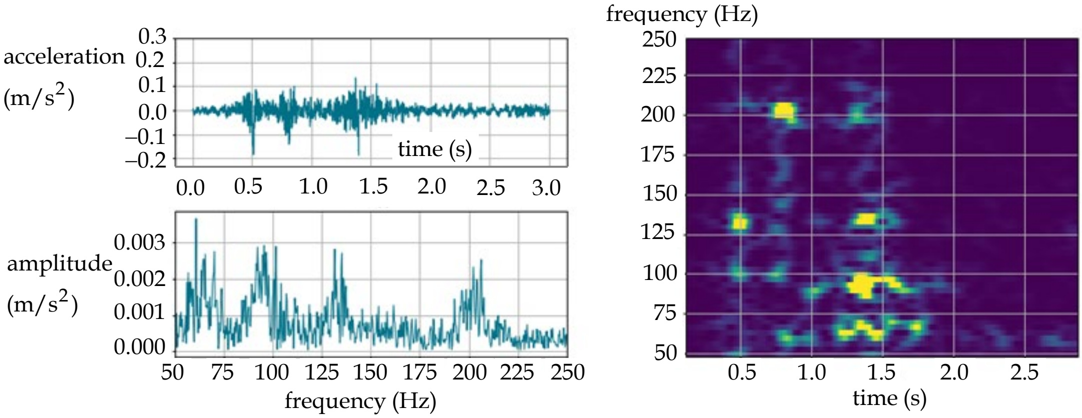

Figure 7. Time history and frequency spectrum (left), and spectrogram (right), of the acceleration response of sensor 17 due to the passage of a semi-trailer truck

4.6 Limitations of data-driven approaches and need for better understanding of the origin of variability

A purely data-driven approach to identify anomalies of bridge deck response from vibration signals would require reliable data normalization procedures. Analysis of measured vibration signals, among which the examples discussed above, yielded the conclusion that this normalisation problem is complex. A better understanding of the nature of bridge deck vibration response variability could potentially be helpful to solve the normalization problem. A simplified semi-analytical model therefore was developed to study the basics of the generation of vibration responses of a supported bending beam loaded by a random moving load of a vehicle passing over an uneven (rough) contact surface.

5 Semi-analytical model

5.1 Model objectives

The objective was to develop a simplified semi-analytical model able to assess local vibration response resulting from moving vehicle loads acting on the system over a much longer length than the deck segment structure spanning between two transverse cross girders. The aim was to investigate with the model the influence of basic moving vehicle parameters on the response characteristics, and to compare the calculated vibration response to characteristic or typical load cases identified from the sensor data. The model was set up to be dimensionless in order to allow for qualitative comparisons of model-based as opposed to measured vibration response, to better understand some of the phenomena observed in the real data.

5.2 *Model definition*

The model setup is summarized here, and schematized in figure 8. For full details the reader is referred to (Kockelkorn, 2022). An Euler-Bernoulli beam of length equal to the full span length of the Haringvliet bridge is modelled, constrained by two pinned supports at its ends,. The beam is supported by dashpots over its full length, representing in simplified form the ability of the actual bridge system to dissipate energy and transfer energy away from the zone of interest. De damping of the viscous beam supports was selected such that a realistic time signal duration and realistic time amplitude characteristics were obtained from the simulations. At mid-span a part of the beam is isolated between two local

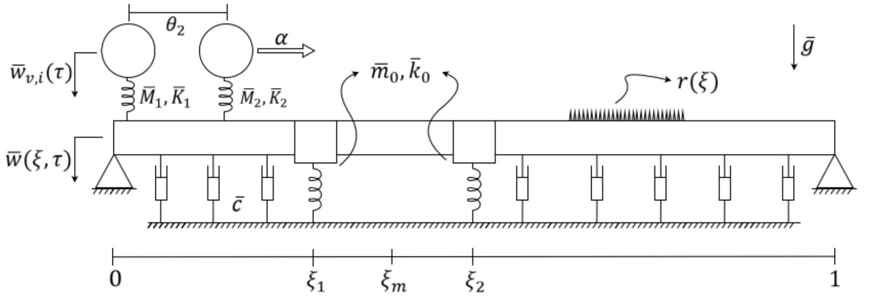

Figure 8: Analytical model configuration with two moving masses

Parameter	Description
ϕ	Angular frequency (rad)
$\bar{w}(\xi,\tau)$	Beam deflection (-)
$\bar{c}$	Beam distributed damping (-)
$\bar{g}$	Gravitational acceleration (-)
$\bar{m}_0$	Resonator mass (-)
$\bar{k}_0$	Resonator spring stiffness (-)
ϕ_s	Sampling frequency (rad)
ξ	Spatial coordinate (-)
τ	Temporal coordinate (-)
η	Unevenness amplitude (-)
κ_i	Unevenness frequency components (-)
$\bar{w}_v(\tau)$	Vehicle deflection (-)
$\bar{M}$	Vehicle mass (-)
$\bar{K}$	Vehicle spring stiffness (-)
α	Vehicle velocity (-)

resonators, of which the stiffness was selected such to be larger than the stiffness of the beam and the moving mass-spring system. By this means the local resonators isolate the part of the beam between them, representing a bridge segment between two transverse cross girders. The beam part between the local resonators is the actual part of interest, where the other parts are just included in the model to be able to simulate the time signature of a passing vehicle over the deck segment of interest. The moving masses represent a vehicle. Combinations of 1 up to 5 moving masses were included in the simulations representing from single axle passages to passages of semi-trailer trucks. The parameters given to the moving loads are mass ratios, stiffnesses, moving velocity and distance between the axles. The load generated by the moving loads acting on the bridge deck is modelled as the result of contact surface unevenness. The unevenness was chosen as to trigger frequencies up to the natural frequencies of the local resonators, taken to be around 100 times the natural frequencies of the moving mass.

The model response is described by the equation of motion of a continuous Euler-Bernoulli beam on continuous viscous supports:

$$\frac{\partial^2}{\partial x^2}\left(EI\frac{\partial^2 w}{\partial x^2}\right)+\rho A\frac{\partial^2 w}{\partial t^2}+c_d\frac{\partial w}{\partial t}=q(x,t) \tag{1}$$

Where x is the spatial coordinate along the beam and $q(x,t)$ refers to an external distributed load on the beam. A dimensionless model is created in order to reduce the amount of input parameters, by setting $x=\xi L$, $w=\overline{w}L$, $w_v=\overline{w}_v L$ and $t=\tau t_0$, where L is the length of the beam. Introducing parameters $t_0=\sqrt{\frac{\rho A}{EI}L^4}$ and $\overline{c}=\frac{c_d L^4}{t_0 EI}$ results in the following equation:

$$\frac{\partial^4\overline{w}}{\partial\xi^4}+\frac{\partial^2\overline{w}}{\partial\tau^2}+\overline{c}\frac{\partial\overline{w}}{\partial\tau}=0 \tag{2}$$

Vehicle action on the system is modelled by moving mass-spring systems, of which the response is described by the following dimensionless equation:

$$\overline{M}\frac{\partial^2\overline{w}_v}{\partial\tau^2}+\overline{K}\overline{w}_v=0\,, \tag{3}$$

in which

$$\overline{M}=\frac{M}{\rho AL}\qquad \overline{K}=\frac{KL^3}{EI} \tag{4}$$

Vibrations of the system are introduced by the forced motion of the moving mass due to the unevenness of the deck surface, triggering vehicle and deck response. Unevenness is defined as the sum of multiple components with random amplitude and phase:

$$r(\xi) = \eta \sum_{i=1}^{M} \varepsilon_i \, s_i \sin\left(\frac{\kappa_i + \delta_i}{\alpha}\xi + \phi_i\right) \tag{5}$$

Where M is the number of unevenness components chosen as 70. Boundary conditions cover the compatibility of deformations at the location of the local resonators. Zero initial conditions are assumed. Combining the beam equation of motion, boundary conditions, the local resonators, unevenness, and the moving mass-spring system results:

$$\begin{aligned} &\frac{\partial^4 \overline{w}}{\partial \xi^4} + \frac{\partial^2 \overline{w}}{\partial \tau^2} + \overline{c}_H \frac{\partial \overline{w}}{\partial \tau} = \\ &= -\left(\delta(\xi - \xi_1) + \delta(\xi - \xi_2)\right)\left(\overline{m}_0 \frac{\partial^2 \overline{w}}{\partial \tau^2} + \overline{k}_0 \overline{w}\right) - \delta(\xi - \alpha\tau)\left(\overline{K}(\overline{w} - \overline{w}_v - r(\xi) - \overline{M}\overline{g}\right) \end{aligned} \tag{6}$$

with

$$\overline{c}_H = \overline{c}\left(H(\xi_1 - \xi) + H(\xi - \xi_2)\right) \tag{7}$$

A general solution was sought by separating variables in the time and spatial domain. Integration over the spatial domain and application of the orthogonality principle results in a system of ordinary differential equation. This system of differential equation is solved numerically by direct time integration using a 7th order Runga-Kutta scheme.

5.3 *Parameter selection*

The model parameters are presented in Table 1. Since we work with a dimensionless model, the parameters cannot directly be linked to physical quantities associated with the actual Haringvliet bridge. The parameters relative to each other are, however, selected such that the system shows behaviour typical for vehicle - bridge interaction. Examples here include a mass ratio of the vehicle relative to the bridge of 5%, local resonator stiffness

Table 1. Model parameters

parameter	value	parameter	value
ξ_1	$38/100$	$\overline{M}$	$5.0\ 10^{-2}$
ξ_2	$45/100$	α	2.0
$\overline{k}_0$	$6.0\ 10^{6}$	$\overline{c}$	$1.0\ 10^{3}$
$\overline{m}_0$	$7.6\ 10^{-2}$	η	$1.0\ 10^{-5}$
$\overline{K}$	$4.0\ 10^{2}$	φ_s	$10000\,\pi$ rad

substantially beyond the beam stiffness, and a level of damping of the viscous supports such that the duration and attenuation of the motion of the bridge part between the local resonators appear realistic. The total set of parameters targets a realistic time domain response of the beam part between the local resonators, similar to recorded motions at the bridge.

5.4 *Modelling of behaviour observed in vehicle passages*

In what follows, attempts are made to generate some signals types that were recurringly observed at the Haringvliet bridge using the semi-analytical model. This allows for interpretations as to the parameters influencing the observed variability of the bridge deck response.

5.4.1 *Doppler effects*

The Doppler effect in the frequency response of the Haringvliet bridge was subsequently simulated with the semi-analytical model presented in the previous sections. The recorded passage of figure 6 could be simulated using the model with two moving masses ($\theta_2 = 0.1$) and the default input parameters. The distance between the masses was chosen large enough to ensure that the masses do not influence each other by the time delay effect, which distorts the signal by either amplifying or damping certain frequencies. The distinctive high-energy frequency bands could be created by amplifying one unevenness frequency component for each moving mass significantly (25 times the original amplitude in this case). The dynamic beam response as calculated using the model is shown in figure 9, and shows strong similarities with the measurements. Again, the influence of the Doppler effect is also visible in the spectrogram of the passage.

As already mentioned above, the Doppler effect was observed in the model when there was a single very dominant unevenness component per axle. The model unevenness describes the roughness and irregularities of the road as well as the roughness of the tyre. Apparently, when the bridge – vehicle interaction results in a very dominant frequency of dynamic loading on the bridge, Doppler-like effects can occur as a result of vibrations, of the crossing vehicles interacting with the bridge, caused by for instance repetitive elements contributing to surface roughness, tyre irregularities or crooked car suspensions.

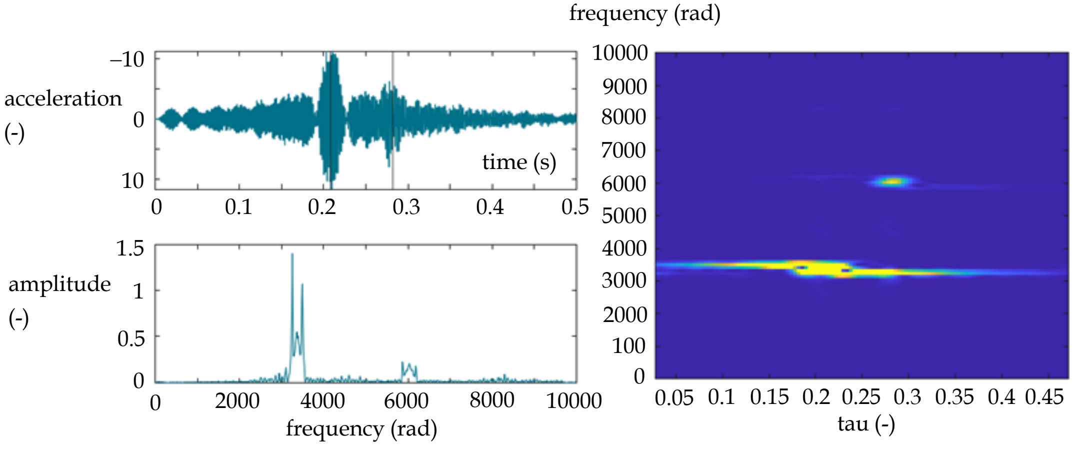

Figure 9. The acceleration response showing the Doppler effect as simulated by the semi-analytical model. Time history and frequency spectrum (left), and spectrogram (right)

5.4.2 Semi-trailer trucks

Also the variability within the semi-trailer truck passages was investigated using the semi-analytical model. Five moving masses were placed on the beam with default model parameters ($\theta_2 = 0.1$, $\theta_3 = 0.24$, $\theta_4 = 0.246$ and $\theta_5 = 0.252$, where θ_n describes the distance between the 1st and nth axle). This resulted in the response shown in figure 10 for two scenarios that differ in terms of the axle loads. Recall that the amplitudes and shapes of the measured and modelled response cannot be directly compared to each other. Yet, the model is able to reasonably describe the variations as seen in the semi-trailer truck passage. As seen in the response of the Haringvliet bridge, multiple high-energy frequency bands appear in the Fourier spectrum of the acceleration response. In addition, the spectrogram shows a significant variation in response for each of the moving masses.

Using the model simulations it was further analysed which factors or mechanisms most likely cause the extremely different frequency response characteristics for signals that appear relatively similar in the time domain. It was concluded that the specific combination of axle configuration, inter-axle distances, and vehicle speed may have a strong effect on the frequency domain response characteristics over time. This is illustrated by the spectrogram plots in figure 11 below. Here spectrograms of the simulated response for two identical vehicles travelling at respectively 50.0 and 37.5 km/h are compared.

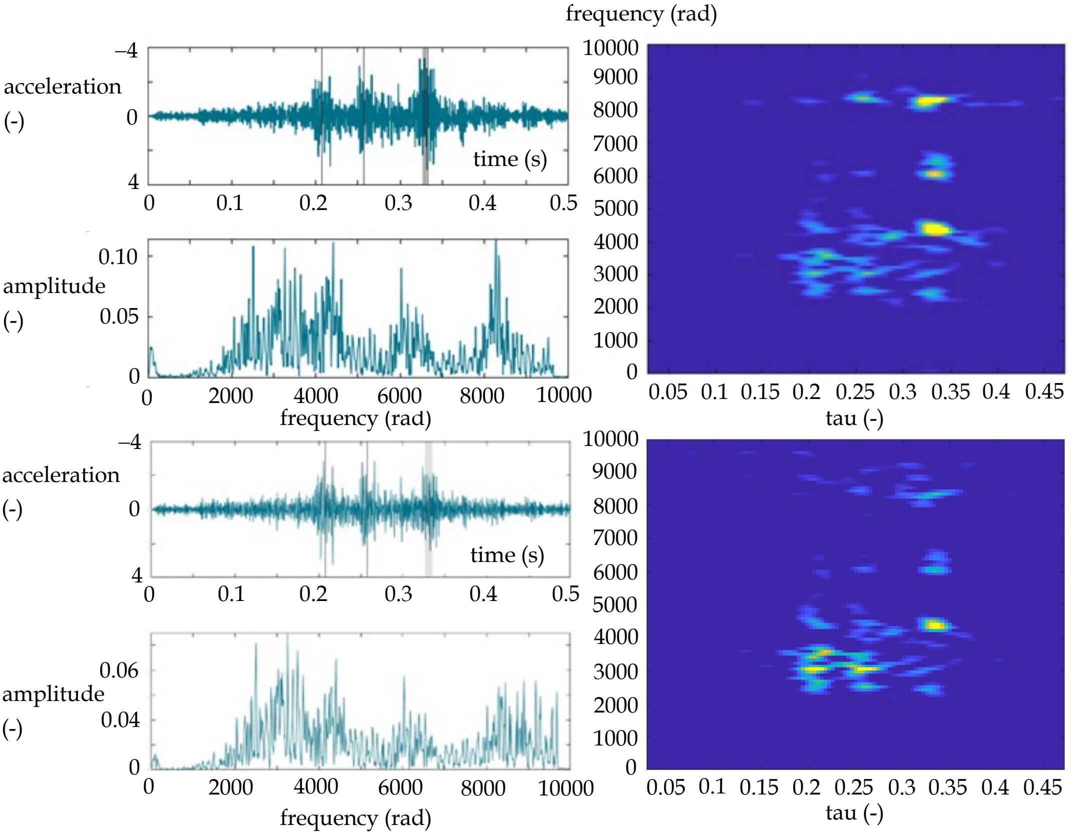

Figure 10. The acceleration response of a semi-trailer truck as simulated by the semi-analytical model. Time history and frequency spectrum (left), and spectrogram (right). Relative axle loads of the 5 semi-trailer truck axles 1:1:1:1:1 (top) and 1:1:0.7:0.7:0.7 (bottom)

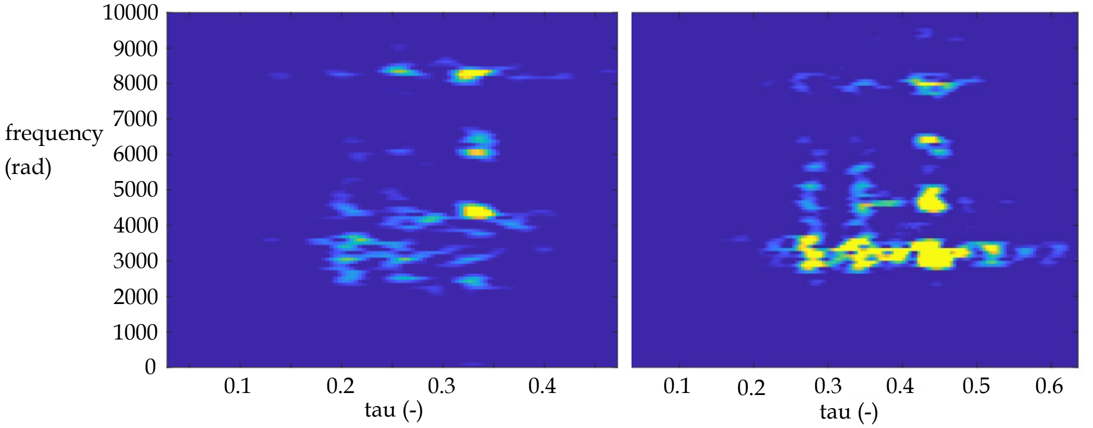

Figure 11. Spectrograms of the simulated response for two identical vehicles at speeds 50.0 and 37.5 km/h, as calculated using the semi-analytical model

6 Conclusions

This paper presented the results of a study on the variability of bridge deck vibrations due to traffic loading. The study combines results from a measurement campaign at the Haringvliet bridge and those of a semi-analytical model. Large variability in the vibration responses is observed from recordings of passing vehicles. This was found to apply to responses of sensors at similar positions for a single passage, as well as to responses recorded using the same sensor for repetitive passages of the same vehicle. The results of the semi-analytical model aided in understanding which parameters are influencing the observed variability – e.g. vehicle speed, axle mass distribution, surface roughness, etc. – and to which extent these parameters could potentially influence the deck vibration response. Future research will focus the definition of damage-sensitive features for structural health monitoring which are less sensitive to variations among individual passages.

Acknowledgements

We acknowledge the inspiring support by Prof. Dr. A.V. Metrikine, who's help was key for the definition and development of the semi-analytical model presented in this paper. The support of Rijkswaterstaat for supplying access to the Haringvliet bridge and funding of the measurement campaign is greatly acknowledged. In particular we would like to express our gratitude to Jaap van der Heide (Rijkswaterstaat) for his efforts to create this opportunity for the team. In addition, we would like to thank Axel Lok (UTwente) for his assistance with the testing and installation of the vibration monitoring system.

References

De Jong, F.B.P (2006). *Renovation techniques for fatigue cracked orthotropic steel bridge decks*, PhD dissertation, Delft University of Technology.

Deraemaeker, A. R. (2012). *New trends in vibration based structural health monitoring*. Springer Science & Business Media, 520.

Deraemaeker, A. R. (2008). Vibration-based structural health monitoring using output-only measurements under changing environment. *Mechanical systems and signal processing*, 22(1), 34-56.

E. J. Cross, G. M. (2012). Features for damage detection with insensitivity to environmental and operational variations. *Proc. R. Soc. A* (468), 4098–4122.

Greijmans, M-L. A. (2020). Vibration-based damage detection of the Haringvlietbrug - A data-driven approach. MSc thesis, Delft University of Technology.

Kockelkorn, T. (2022). Dynamic response of an orthotropic bridge deck subjected to EOVs: A case study of the Haringvliet bridge. MSc thesis, Delft University of Technology.

Kortendijk, C. N. (2021). Characterizing the effect of environmental variability on local vibrations: experiences on the Haringvliet bridge. *10th International Conference on Structural Health Monitoring of Intelligent Infrastructure*.

Maes, K. V. (2022). Validation of vibration-based structural health monitoring on retrofitted railway bridge KW51. *Mechanical Systems and Signal Processing,* 165, 108380.

Sohn, H. (2017). Effects of Environmental and Operational Variability on Structural Health Monitoring. *Phil. Trans. R. Soc. A*, 365, 539-560.

Ya, S. et al. (2011). Fatigue Evaluation of Rib-to-Deck Welded Joints of Orthotropic Steel Bridge Deck. *Journal of Bridge Engineering* 16.4, 492–499.